Journal of Peptide Science
J. Peptide Sci. **8**: 476–488 (2002)
Published online in Wiley InterScience (www.interscience.wiley.com). DOI: 10.1002/psc.410

Conformational Analysis of the $G\alpha_s$ Protein *C*-Terminal Region

ANNA MARIA D'URSI,[a] STEFANIA ALBRIZIO,[b] GIOVANNI GRECO,[b] SONIA MAZZEO,[a] MARIA R. MAZZONI,[c] ETTORE NOVELLINO[b] and PAOLO ROVERO[a]*

[a] Dipartimento di Scienze Farmaceutiche, Università di Salerno, Salerno, Italy
[b] Dipartimento di Chimica Farmaceutica e Tossicologica, Università di Napoli 'Federico II', Napoli, Italy
[c] Dipartimento di Psichiatria, Neurobiologia, Farmacologia e Biotecnologie, Università di Pisa, Pisa, Italy

Received 29 January 2002
Accepted 29 April 2002

Abstract: The *C*-terminal domain of the heterotrimeric G protein α-subunits plays a key role in selective activation of G proteins by their cognate receptors. Several *C*-terminal fragments of $G\alpha_s$ (from 11 to 21 residues) were recently synthesized. The ability of these peptides to stimulate agonist binding was found to be related to their size. $G\alpha_s(380–394)$ is a 15-mer peptide of intermediate length among those synthesized and tested that displays a biological activity surprisingly weak compared with that of the corresponding 21-mer peptide, shown to be the most active. In the present investigation, $G\alpha_s(380–394)$ was subjected to a conformational NMR analysis in a fluorinated isotropic environment. An NMR structure, calculated on the basis of the data derived from conventional 1D and 2D homonuclear experiments, shows that the *C*-terminal residues of $G\alpha_s(380–394)$ are involved in a helical arrangement whose length is comparable to that of the most active 21-mer peptide. A comparative structural refinement of the NMR structures of $G\alpha_s(380–394)$ and $G\alpha_s(374–394)C^{379}A$ was performed using molecular dynamics calculations. The results give structural elements to interpret the role played by both the backbone conformation and the side chain arrangement in determining the activity of the G protein *C*-terminal fragments. The orientation of the side chains allows the peptides to assume contacts crucial for the G protein/receptor interaction. In the 15-mer peptide the lack as well as the disorder of some *N*-terminal residues could explain the low biological activity observed.

Keywords: conformation; $G\alpha_s$ peptides; NMR; structure

Abbreviations: CD, circular dichroism; Fmoc, 9-fluorenylmethoxycarbonyl; DQF-COSY, double quantum filtered correlated spectroscopy; TOCSY, total correlated spectroscopy; $G\alpha$ and $G\beta\gamma$, the α and $\beta\gamma$ subunits of heterotrimeric G proteins; G_s, a G protein linked with the activation of adenylyl cyclase; $G\alpha_s$, the α subunit of G_s; G_i, a G protein linked with the inhibition of adenylyl cyclase; $G\alpha_i$, the α subunit of G_i; G_t (or transducin), the G protein present in rod outer segments; $G\alpha_t$, the α subunit of G_t; $G\alpha_s(374–394)C^{379}A$, a synthetic peptide corresponding to those residues of $G\alpha_s$ with a cysteine substituted by an alanine (a $G\alpha$ subunit followed by numbers refers to the corresponding peptide); GTPγS, guanosine-5'-*O*-(3-thiotriphosphate); HFA, hexafluoroacetone; HPLC, high-performance liquid chromatography; MD, molecular dynamics; NMR, nuclear magnetic resonance; NOE, nuclear Overhauser effect; NOESY, nuclear Overhauser enhancement spectroscopy.

*Correspondence to: Paolo Rovero, Dipartimento di Scienze Farmaceutiche, Università di Salerno, Salerno, Italy; e-mail: rovero@unisa.it

Contract/grant sponsor: Human Capital and Mobility grant, European Community; Contract/grant number: (CHRX-CT94-0689).
Contract/grant sponsor: Regione Campania; Contract/grant number: POP 1996-2000.
Contract/grant sponsor: Ministero Università Ricerca Scientifica e Tecnologica; Contract/grant number: PRIN 2000.

INTRODUCTION

A large number of hormones, neurotransmitters, chemokines, local mediators and sensory stimuli exert their effects on cells by binding to diverse heptahelical cell surface receptors. The heterotrimeric guanine nucleotide-binding regulatory proteins (G proteins, $G\alpha\beta\gamma$) mediate signalling from these receptors to a variety of intracellular effectors [1]. These pathways control numerous essential functions in all tissues and are ubiquitous throughout eukaryotes. Heterotrimeric G proteins have been proposed as new targets for specific antagonists of signal transduction pathways [2].

The role of various G protein domains for receptor interaction has been defined on the basis of site directed mutagenesis, chimeric protein and peptide experiments [3–20]. Although the heterotrimeric G protein ($G\alpha$ and $G\beta\gamma$ subunits) is required for an effective coupling with the receptor, the *C*-terminal domain of $G\alpha$ subunits plays a pivotal role in ensuring receptor G protein interaction and signal transduction [3,4,7,9,13,15,18,20].

Despite the fact that some theoretical models of receptor/G protein interaction have been elaborated, emphasizing the concept of the low specificity of this coupling [21], the molecular determinants of receptor/G protein interaction seem to vary somewhat among specific families of receptors and G proteins. Consistently, it has been demonstrated that the *C*-terminal region of $G\alpha$ subunits is central in mediating receptor G protein selectivity [3,4,7]. Substitution of three to five *C*-terminal amino acids of $G\alpha_q$ with the corresponding residues from $G\alpha_i$ allows receptors that normally signal exclusively through $G\alpha_i$ subunits to activate the chimeric $G\alpha_q/G\alpha_i$ subunits and stimulate the G_q effector, phospholipase *C*-β [3].

While a plethora of biochemical data converge on the role of the $G\alpha$ *C*-terminus supporting the specificity of the receptor/G protein interactions, data from structural studies are not exhaustive and show contradictory results. Crystal structures of $G\alpha_t$, $G\alpha_i$ and $G\alpha_s$ [22–26] show that the *C*-terminal region of $G\alpha$ subunits is arranged in an α-helical structure. However, the last three ($G\alpha_s$) to eight ($G\alpha_i$ and $G\alpha_t$) residues are disordered in these structures. NMR studies [27] of a $G\alpha_t$ *C*-terminal undecapeptide, $G\alpha_t(340–350)K^{341}R$, have shown that the conformation of the last residues is disordered in the presence of dark rhodopsin while they form a β-turn when bound to the photoisomerized rhodopsin, metarhodopsin II. On the other hand, a more recent NMR investigation [28] indicates that in the presence of photoisomerized rhodopsin the $G\alpha_t$ *C*-terminal undecapeptide is completely ordered and it is arranged in an α-helical structure extending the helix $\alpha5$ of the protein.

To explore the dependence of both activity and conformational propensity on the length of the *C*-terminal region of the $G\alpha_s$ subunit, we have recently synthesized several fragments (from 11 to 21 residues) regularly spaced by two residue increments. The ability of these peptides to stimulate agonist binding was found to be related to their size: peptides containing 17 to 21 residues proved to be more active, while the 11-, 13- and 15-residue peptides were the least effective. In particular, the 13-mer peptide showed a minimum of activity when assayed in the presence of GTPγs [20]. While the biological activity was tested for all of them, the conformation was examined only at the two extremes, namely the 11-mer and the 21-mer peptides [20,29]. When studied in 50/50 (v/v) water/HFA, by NMR, the 11-mer, $G\alpha_s(384–394)$ and the 21-mer, $G\alpha_s(374–394)C^{379}A$, exhibited a helical conformation involving five and eleven *C*-terminal residues, respectively. The conformational data were correlated to the biological results assuming that the pharmacological activity is dependent on the structural regularity of the peptides and thus on the length of their sequences. On this basis, a dependence of biological activity on the ability of peptides to assume an ordered backbone structure was postulated. In conflict with this hypothesis, a glance at the biological data shows that the activity of the 15-mer peptide, whose dimension is intermediate between the 11-mer and the 21-mer, is comparable to that of the least effective peptide, namely the 11-mer [20]. Here we present a structural investigation by NMR spectroscopy of the 15-mer $G\alpha_s(380–394)$. Starting from NMR data a structural refinement was performed by means of a molecular dynamics calculation. The results give new elements to understand which proportion of the interaction of the $G\alpha_s$ peptides with the intracellular portion of the receptor depends on the stability of the helical stretch, on its length or on a specific arrangement of side chains.

MATERIALS AND METHODS

Peptide Synthesis

Peptides were synthesized by the continuous-flow solid-phase method using Fmoc chemistry

on a Milligen 9050 automatic synthesizer. Crude peptides were purified by reverse-phase HPLC on a preparative Vydac C_{18} column (2.2×25 cm) using a 15%–30% gradient of acetonitrile in 0.1% trifluoroacetic acid-water (v/v). Analytical data were reported elsewhere [20].

Circular Dichroism Spectroscopy

All CD spectra were recorded on a Jasco J-710 spectropolarimeter using cells of 1 mm pathlength. The pH of the samples was adjusted to 6.6 with aqueous phosphate buffer. After pH adjustment, samples were lyophilized and dissolved in water or in two different aqueous solutions containing 50% (v/v) methanol or HFA to obtain a peptide concentration of 2×10^{-4} M. Peptide concentrations were determined using the single tyrosine absorbance at 280 nm ($\varepsilon_{280\text{nm}} = 1400\ \text{M}^{-1}\ \text{cm}^{-1}$). Spectra were the average of two scans from 190 to 260 nm, recorded with a band width of 0.5 nm at scan rate of 5 nm/min.

NMR Spectrometry

Samples for NMR were prepared by dissolving 1.2 mg of Gα_s(380–394) and 1.5 mg of Gα_s(374–394)C^{379}A in 0.5 ml of H_2O phosphate buffer (pH 6.6). Samples were lyophilized and dissolved in an aqueous solution containing 50% (v/v) HFA. NMR spectra were recorded on a Bruker DRX-600 spectrometer. One-dimensional (1D) NMR spectra were recorded in the Fourier mode with quadrature detection. The water signal was suppressed by a low-power selective irradiation in the homogated mode. DQF-COSY [30], TOCSY [31] and NOESY [32] experiments were run in the phase-sensitive mode using quadrature detection in ω_1 by time-proportional phase incrementation of the initial pulse [33]. Data block sizes comprised 2048 addresses in t_2 and 512 equidistant t_1 values. Before Fourier transformation, the time domain data matrices were multiplied by shifted $\sin^2$ functions in both dimensions. A mixing time of 70 ms was used for the TOCSY experiments. NOESY experiments were run at 300 K with mixing times in the range 100–250 ms. The qualitative and quantitative analyses of DQF-COSY, TOCSY and NOESY spectra were obtained using the XEASY interactive program package [34].

NMR Structure Calculation

On the basis of 241 NOE derived distances 3D models of Gα_s(380–394) were generated with a simulated annealing procedure using the DYANA software package [35]. The NOE derived restraints were distributed as 110 intraresidue, 61 short-range, 68 medium-range and 2 long-range constraints. All structures were energy minimized with the SANDER module of the AMBER 5 program [36,37] using for 1000 steps the steepest descent method and for 4000 steps the conjugate gradient method. A non-bonded cut-off of 12 Å and a distance-dependent dielectric term ($e = 4 * r$) were used. The minimization protocol included three steps in which NOE derived distances were used as constraints with a force constant, respectively, of 1000, 100 and 10 kcal/molÅ. The final *pdb* file was subjected to a PROCHECK [38] protocol for a validation of the geometry.

Molecular Dynamics

Molecular dynamics runs were performed using the SANDER module of the AMBER 5 software at a constant temperature of 300 K, using a nonbonded cut-off of 12 Å and a distance-dependent dielectric term ($e = 4 * r$). NMR mean structures of Gα_s(380–394) and Gα_s(374–394) were chosen as starting structures. The molecular dynamics simulations were performed with a rather drastic limitation of allowed movements for backbone atoms, whereas side-chain atoms were allowed to move according to a small value of force constant restraints. A force constant of 1000 kcal/mol Å was applied on the NOE derived distance restraints of the backbone atoms, whereas a force constant of 10 kcal/mol Å was used to constrain side-chain atoms. After 1 ps of heating and 10 ps of initialization time, the system was subjected to a 500 ps simulation with 1 fs time steps. Structures were saved every 5 ps. The average AMBER energy was −1223 Kcal/mol and −1180 Kcal/mol for Gα_s(374–394)C^{379}A and Gα_s(380–394), respectively. The all atoms root mean square deviation (RMSD) from the start of the trajectory was 1.1 Å for Gα_s(374–394)C^{379}A structure and 1.25 Å for the Gα_s(380–394) structure. The final structures were analysed using the Insight 98.0 program (Molecular Simulations, San Diego, CA) [39].

RESULTS

CD and NMR Analysis

A preliminary screening of the conformational preferences of Gα_s(380–394) as a function of the

environment was performed by means of CD spectroscopy. The spectrum in water (pH 6.6) presented a negative band at 201 nm that is characteristic of a random coil structure. This suggests that $G\alpha_s(380–394)$, like most short linear peptides, assumes an unordered conformation under these conditions.

The CD spectra of $G\alpha_s(380–394)$ recorded in 50/50 water/methanol (v/v) and 50/50 water/HFA (v/v) mixtures [40,41] show the double-well shape typical of right-handed α-helical structures including negative bands at 208 and 222 nm and an additional positive signal at 192 nm. In Figure 1 the CD spectra of $G\alpha_s(380–394)$ and $G\alpha_s(374–394)C^{379}$ in 50/50 water/HFA (v/v) are reported. Consistent with its exceptional helix inducing properties, the HFA/water mixture favours the highest α-helix content. A single value deconvolution method [42] gave a global result of 32% α-helices, 4% β-strands, 33% β-turns and 31% random coil in the water/methanol mixture, whereas amounts of 40% α-helices, 5% β-strands, 31% β-turns and 24% random coil in the HFA/water mixture.

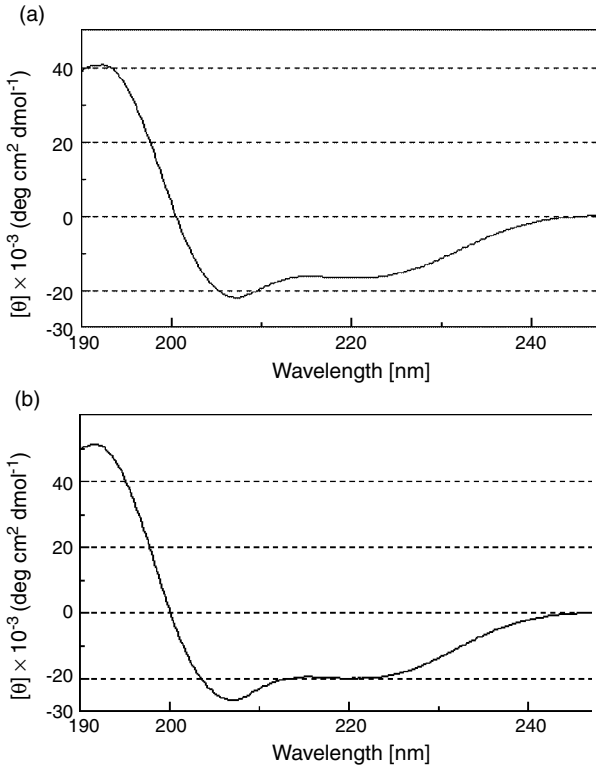

Figure 1 Circular dichroism spectra of $G\alpha_s(380–394)$ (a) and $G\alpha_s(374–394)C^{379}A$ (b) recorded at room temperature in 50/50 water/HFA (v/v). Peptide concentration was 2×10^{-4} M.

NMR spectra were acquired in the three solvent media water, 50/50 water/methanol (v/v) and 50/50 water/HFA (v/v). Chemical shift assignments of $G\alpha_s(380–394)$ proton spectra were achieved via the standard systematic application of DQF-COSY [30], TOCSY [31] and NOESY [32] experiments, using the XEASY [34] software package according to the procedure of Wüthrich [43].

Data collected in the water/HFA mixture showed the most complete pattern of helical secondary structure, confirming the preliminary CD data. To exclude problems deriving from aggregation, 1D proton spectra in the 50/50 water/HFA (v/v) mixture were recorded in a range of concentrations from 1 mM to 0.1 mM. In 50/50 water/HFA (v/v), at a peptide concentration of 0.1 mM, the peptides did not display any noticeable effects of aggregation. The values of the proton chemical shifts of $G\alpha_s(380–394)$ and $G\alpha_s(374–394)C^{379}$ A are reported in Table 1. The Hα chemical shifts present a remarkable upfield shift compared with the standard values reported for random coil conformations [44]. In Figure 2 the chemical shift indexes for $G\alpha_s(380–394)$ and for $G\alpha_s(374–394)C^{379}A$ are reported. According to the chemical shift index (CSI) grouping of four (not necessarily consecutive) '−1s' is needed to define turn-helix conformations. Regions characterized by non consecutive '0s' or '1s' are designated as coils. [44,45]. As it is evident in Figure 2, both peptides show '−1s' values of chemical shift indexes in similar positions of the sequences; this finding is suggestive of the presence of turn-helix conformation in the same portion of the sequences. Furthermore, the extension of regions characterized by '−1' values of CSI shows that the size of the turn-helix conformation is proportional to the length of the peptides. Values 0 or +1 are present at the terminal part of both peptides, thus suggesting a prevalence of disordered conformations in these regions.

The amide and fingerprint regions of NOESY spectra of $G\alpha_s(380–394)$ collected in water/HFA are reported in Figure 3. A high number of well resolved cross peaks are visible, indicating the presence of highly represented, ordered conformers.

The diagnostic sequential and medium-range connectivities of $G\alpha_s(380–394)$ are reported in Figure 4. Analysis of the diagram shows that the *N*-terminal part of the peptide lacks medium-range NOEs, while it is characterized by a series of sequential αCH_i-NH_{i+1} NOEs, consistent with a mixture of poorly structured or flexible regions.

Table 1 Relevant Proton Chemical Shifts of $G\alpha_s(374–394)C^{379}A$ and $G\alpha_s(380–394)$ in 50 : 50 Water/HFA (v/v), at 600 MHz and 300 K

Residue	Peptide	NH	CHα	Hβ	Hγ	Hδ	Hε	Others
Arg^{374}	$G\alpha_s(374–394)C^{379}A$		4.06	1.88/1.90	1.48/1.90	3.13/3.15		
Val^{375}	$G\alpha_s(374–394)C^{379}A$	8.30	4.19	2.06				$\gamma CH_3$0.67/0.90
Phe^{376}	$G\alpha_s(374–394)C^{379}A$	7.97	4.69	2.97/2.68		7.30	7.26	Hz 7.36
Asn^{377}	$G\alpha_s(374–394)C^{379}A$	8.87	4.68	2.86/2.95				Hδ 7.17 Hε 7.42
Asp^{378}	$G\alpha_s(374–394)C^{379}A$	8.05	4.68	3.02/3.00				
Ala^{379}	$G\alpha_s(374–394)C^{379}A$	8.14	4.18	1.53				
Arg^{380}	$G\alpha_s(374–394)C^{379}A$	8.47	3.97	1.79/1.97	1.67/1.69	3.24/3.26	7.14	
	$G\alpha_s(380–394)$	8.10	4.18	1.96/2.04	1.82/1.80	3.27/3.29	7.20	
Asp^{381}	$G\alpha_s(374–394)C^{379}A$	8.21	4.66	2.97/2.99				
	$G\alpha_s(380–394)$	8.64	4.97	2.91/2.98				
Ile^{382}	$G\alpha_s(374–394)C^{379}A$	7.59	3.83	2.14	1.64/1.66			γCH_3 1.04 δCH_3 0.91
	$G\alpha_s(380–394)$	7.95	4.08	1.97	1.56/1.58			γCH_3 1.18 δCH_3 1.05
Ile^{383}	$G\alpha_s(374–394)C^{379}A$	8.17	3.81	1.96	1.29/1.31			γCH_3 1.00 δCH_3 0.90
	$G\alpha_s(380–394)$	7.83	3.96	2.02	1.64/1.66			γCH_3 1.18 δCH_3 1.00
Gln^{384}	$G\alpha_s(374–394)C^{379}A$	8.37	4.13	2.39/2.42	2.40/2.66			7.03/7.08
	$G\alpha_s(380–394)$	8.41	4.06	2.26/2.28	2.47/2.51			6.61/7.03
Arg^{385}	$G\alpha_s(374–394)C^{379}A$	7.96	4.12	1.99/2.06	1.78/1.80	3.21/3.23	7.11	
	$G\alpha_s(380–394)$	8.01	4.08	2.00/2.02	1.72/1.85	3.19/3.21	7.10	
Met^{386}	$G\alpha_s(374–394)C^{379}A$	8.76	4.23	2.31/2.33	2.61/2.83			
	$G\alpha_s(380–394)$	8.49	4.25	2.13/2.28	2.62/2.68			
His^{387}	$G\alpha_s(374–394)C^{379}A$	8.20	4.42	3.42/3.44				2H 7.40 4H 8.36
	$G\alpha_s(380–394)$	8.16	4.43	3.38/3.40				2H 7.38 4H 8.41
Leu^{388}	$G\alpha_s(374–394)C^{379}A$	8.20	4.32	1.85/1.95	1.87			δCH3 0.69/0.72
	$G\alpha_s(380–394)$	8.14	4.31	1.80/1.82	1.89			δCH3 0.96/0.98
Arg^{389}	$G\alpha_s(374–394)C^{379}A$	8.22	4.20	2.00/2.06	1.79/1.81	3.33/3.35	7.12	
	$G\alpha_s(380–394)$	8.11	4.16	1.96/2.03	1.77/1.79	3.31/3.33	7.10	
Gln^{390}	$G\alpha_s(374–394)C^{379}A$	7.92	4.11	2.10/2.12	2.31/2.38			6.59/7.03
	$G\alpha_s(380–394)$	7.96	4.10	2.10/2.12	2.29/2.37			6.61/7.00
Tyr^{391}	$G\alpha_s(374–394)C^{379}A$	7.96	4.49	3.13/3.32		7.20	6.87	
	$G\alpha_s(380–394)$	7.94	4.47	3.11/3.28		7.18	6.86	
Glu^{392}	$G\alpha_s(374–394)C^{379}A$	8.16	4.26	2.26/2.28	2.54/2.56			
	$G\alpha_s(380–394)$	8.13	4.25	2.25/2.27	2.58/2.65			
Leu^{393}	$G\alpha_s(374–394)C^{379}A$	7.77	4.42	1.71/1.85	1.81			δCH_3 0.95/0.97
	$G\alpha_s(380–394)$	7.76	4.40	1.69/1.80	1.82			δCH_3 0.93/0.95
Leu^{394}	$G\alpha_s(374–394)C^{379}A$	7.51	4.35	1.70/1.79	1.81			δCH_3 0.65/0.68
	$G\alpha_s(380–394)$	7.56	4.38	1.68/1.81	1.79			δCH_3 0.93/0.95

All values refer to water residue signal.

The region Ile^{382}–Leu^{394} shows a well defined helical structure, as suggested by the presence of dNN(i, i + 1) sequential connectivities and numerous dαN(i, i + 3), d$\alpha\beta$(i, i + 3), and dαN(i, i+4) medium-range connectivities.

$G\alpha_s(380–394)$ NMR Structure Calculations

Three-dimensional structures of $G\alpha_s(380–394)$ were calculated by simulated annealing procedures based on 241 NOE-derived restraints. The best 20 structures of 50 calculated were chosen according to the lowest values of the penalty (f) for the target function [35]. These structures were energy minimized using the distance restraints with a progressively smaller force constant. The minimization procedure yielded an improved helical geometry and a lower total energy of the structures. To validate the resulting structures the *pdb* files were submitted to an online PROCHECK procedure [38]. Table 2 reports the backbone torsion angles of $G\alpha_s(380–394)$. The

Ramachandran plot shows a distribution of eight couple of backbone dihedral angles in regions corresponding to core helical structures and four couples of angles in regions corresponding to allowed helical regions. These results are consistent with a helical geometry spanning from Ile^{383} to His^{387} and from Arg^{389} to Leu^{393}.

Plate 1a reports an overlap of the 20 best structures of $G\alpha_s(380–394)$ as calculated from DYANA and then minimized with the SANDER module of the AMBER 5 software package. In agreement with the NOESY data, the structure bundle shows the presence of disordered conformations in the *N*-terminal regions, whereas ordered conformations are observable in the central and *C*-terminal regions. The backbone RMSD was 0.57Å in the *C*-terminal region. In Plate 1b the backbone of the best 20 $G\alpha_s(380–394)$ structures is overlapped to the backbone of the corresponding regions of the $G\alpha_s(374–394)C^{379}A$ peptide [20] and $G\alpha_s$ crystal structure (ref. code 1AZT) [26]. High agreement for the two sets of structures is observed in the 11 *C*-terminal residues.

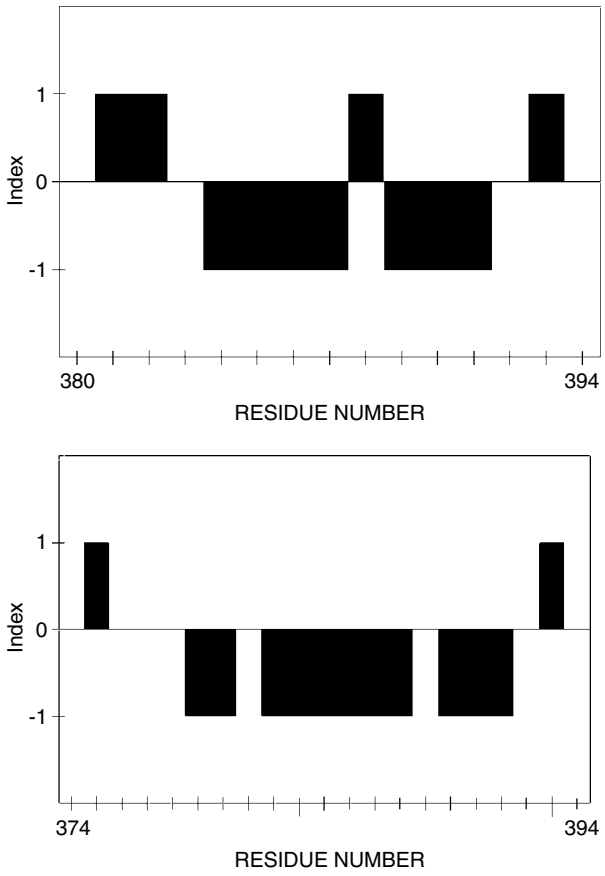

Figure 2 The αCH chemical shift indexes for $G\alpha_s(380–394)$ (top) $G\alpha_s(374–394)C^{379}A$ (bottom) in 50/50 HFA/water (v/v) at 300 K.

Molecular Dynamics Refinement

To characterize the spatial region occupied by the peptide side chains, a 500 ps molecular dynamics simulation was performed, starting from the $G\alpha_s(380–394)$ and $G\alpha_s(374–394)C^{379}A$ mean structures. The molecular dynamics simulation was performed with a rather drastic limitation of allowed movements for backbone atoms, whereas side chain atoms were allowed to move according to a small value of force constant restraints (see Materials and Methods).

Side chains are well defined in both models, but the 21-mer $G\alpha_s(374–394)C^{379}A$ shows a better structural definition as compared to that of 15-mer. Accordingly, Plate 2 shows a superposition of $G\alpha_s(374–394)C^{379}A$ structures collected every 5 ps during the last 50 ps of molecular dynamics simulation. Several side chains are displayed and coloured according to their hydrophobic character. They occupy narrow spatial regions. The orientation of the side chains suggests the presence of a polar surface defined by functionally relevant negative charged residues (Asp^{378}, Asp^{381}) which are stabilized by the spatial proximity of positive charged Arg^{380} and Arg^{385}. On the other hand, hydrophobic surfaces are defined by residues exhibiting less polar side chains (His^{387}, Tyr^{391}) and apolar side chains (Ile^{382}, Ile^{383}, Met^{386}, Leu^{393}). In Plate 3 the helix $\alpha1$ and the helix $\alpha5$ of the crystal model (ref. code 1AZT) of the $G\alpha_s$ protein are displayed [26]. The atoms involved in the interaction have been outlined by defining a subset including all atoms positioned in a range of 5 Å from helix $\alpha5$. The last ten *C*-terminal residues of helix $\alpha5$ of the crystal structure are displayed exhibiting their side chains, and they are fitted on the backbone heavy atoms of the corresponding regions of $G\alpha_s(374–394)C^{379}A$ structure. A comparison of the side chain orientations of the mentioned segments indicates that the spatial regions occupied by these side chains are common. In particular, in the structures of $G\alpha_s(374–394)C^{379}A$ the side chains of Ile^{383}, Gln^{384}, His^{387} and Tyr^{391} are in good agreement with those of the intact protein that are rightly oriented to interact with helix $\alpha1$ [20]. On the other hand, the side chains of Ile^{382}, $Met^{386}$and Leu^{393} are exposed for a possible interaction with

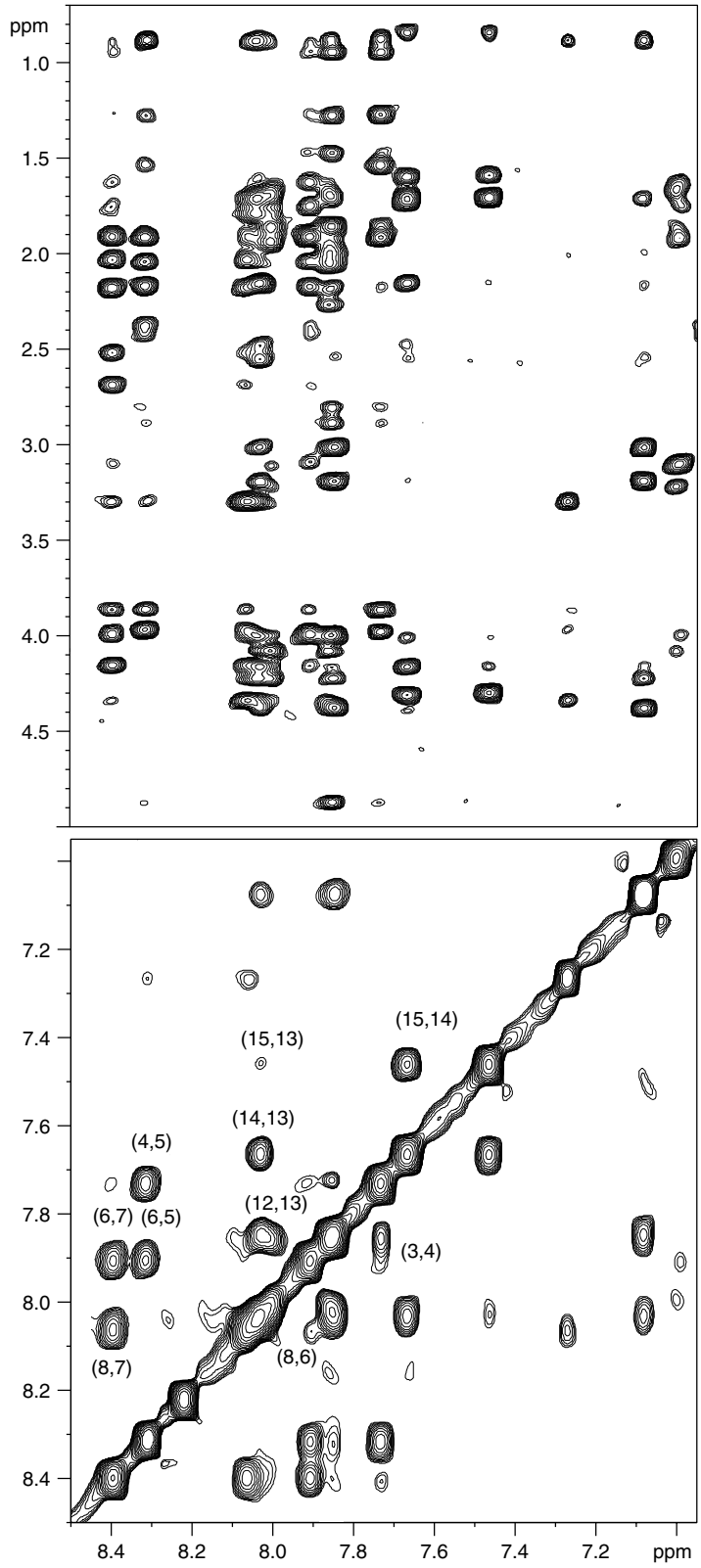

Figure 3 Fingerprint region (top) and amide region (bottom) of the NOESY spectra of Gα_s(380–394) in 50/50 HFA/water (v/v). (600 MHz.; T = 300 K, 1.8 mM). Several sequential cross peaks are labelled.

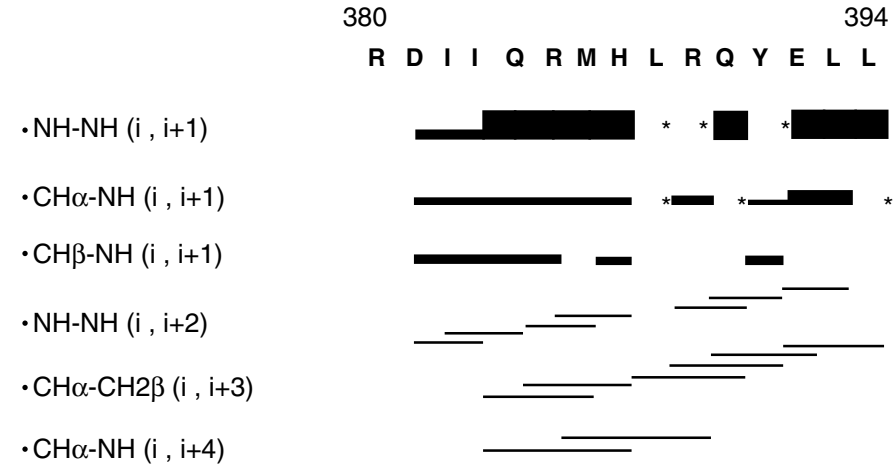

Figure 4 Sequential and medium-range NOEs for $G\alpha_s(380–394)$. Data were obtained from a 600 MHz NOESY experiment with a mixing time of 150 ms and collected in 50/50 water/HFA (v/v) at 300 K.

the *C*-terminal helix of the cognate receptor [21]. Due to the size of the 15-mer, in the models of $G\alpha_s(380–394)$ a good agreement with the side chains of helix $\alpha 5$ and $G\alpha_s(374–394)C^{379}A$ is possible only in the very last *C*-terminal residues. It seems that the structural arrangement of $G\alpha_s(380–394)$ is such that some important side-chain contacts are missing.

DISCUSSION

Many biological and structural data [3, 4, 7, 9, 13, 15, 18, 20] suggest an important role for the $G\alpha$ *C*-terminal domain in regulating the coupling process of G proteins with their cognate receptors, although the structural determinants of receptor/G protein interactions have not yet been determined. Various models of interaction have been elaborated [22,26] on the basis of crystallographic data. The limitation of these data is that the coordinates of the three *C*-terminal residues are missing [22,26,27], whereas one of the last three *C*-terminal residues is Leu^{393}, which is a highly conserved residue, considered essential for the coupling process. Therefore, the conformational analysis in solution of synthetic peptides that belong to this region is gaining increased importance.

We have recently synthesized several peptide fragments (from 11 to 21 residues, regularly spaced by two residue increments) corresponding to the *C*-terminal region of the $G\alpha_s$ subunit [20]. While the ability to interfere with A_{2a} adenosine receptor signal transduction [20] was tested for all of them, the conformation in solution was examined only for the 11-mer and the 21-mer peptides. These fragments were chosen as representatives of the two levels of activity detected, according to the observation that the 11-, 13- and 15-residue peptides were the least biologically active, while the 17-, 19- and 21-residue peptides were the most active. The 11-mer $G\alpha_s(384–394)$ and the 21-mer $G\alpha_s(374–394)C^{379}A$, studied by NMR, fold into a regular helix in 50/50 HFA/water (v/v). These helical segments are made

Table 2 Values of the ϕ and ψ Dihedral Angles for the $G\alpha_s(380–394)$ Structure as Derived from 50/50 NMR Data in Water/HFA (v/v), at 600 MHz and 300 K

Residue	ψ	ϕ
Arg^{380}	139.7 ± 49	
Asp^{381}	-170.6 ± 30	-85.0 ± 33
Ile^{382}	-19.3 ± 34	-116.3 ± 50
Ile^{383}	-7.4 ± 27	-6.1 ± 39
Gln^{384}	-41.4 ± 19	-78.3 ± 29
Arg^{385}	-28.5 ± 12	-78.7 ± 25
Met^{386}	-24.4 ± 16	-65.7 ± 15
His^{387}	17.8 ± 13	-117.0 ± 12
Leu^{388}	-7.2 ± 12	-74.1 ± 27
Arg^{389}	-15.1 ± 12	-78.8 ± 14
Gln^{390}	-14.4 ± 12	-80.2 ± 15
Tyr^{391}	-20.1 ± 11	-79.9 ± 16
Glu^{392}	39.3 ± 13	-93.4 ± 18
Leu^{393}	30.5 ± 10	-153.2 ± 27
Leu^{394}		-83.6 ± 32

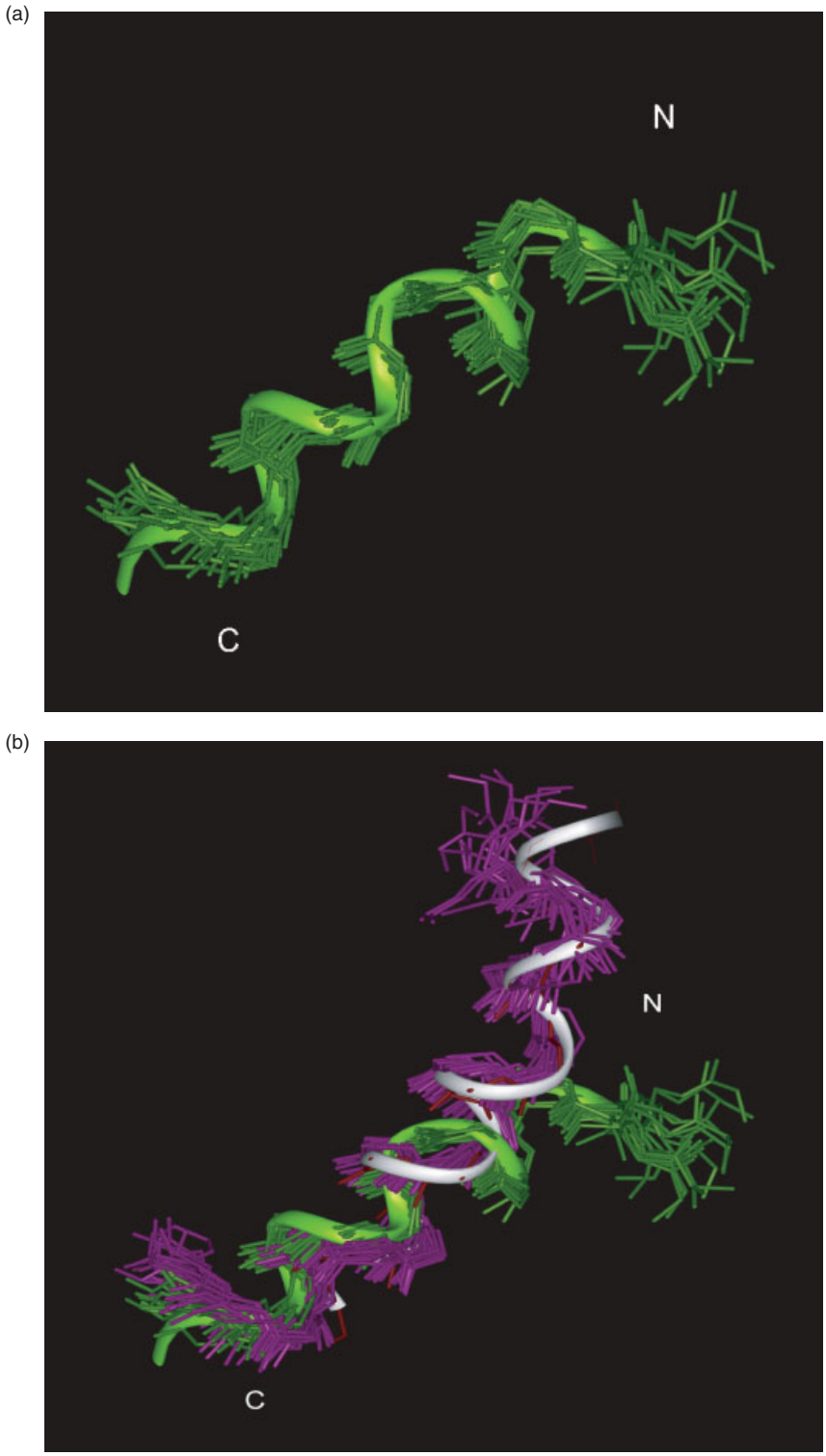

Plate 1 (a) The best 20 calculated structures of $G\alpha_s(380–394)$ (green) as derived from DYANA calculations and energy minimized using the SANDER module of AMBER 5 software. The structures are fitted on the backbone heavy atoms of the Ile^{382}-Leu^{394} segment. (b) Backbone conformations of $G\alpha_s(380–394)$ (green) and $G\alpha_s(374–394)C^{379}A$ (purple) superimposed on the crystallographic structure of the same fragment in the $G\alpha_s$ protein (white ribbon) [26]. The segment Glu^{392}-Leu^{394} of the protein is not displayed since its coordinates are not reported in the PDB file.

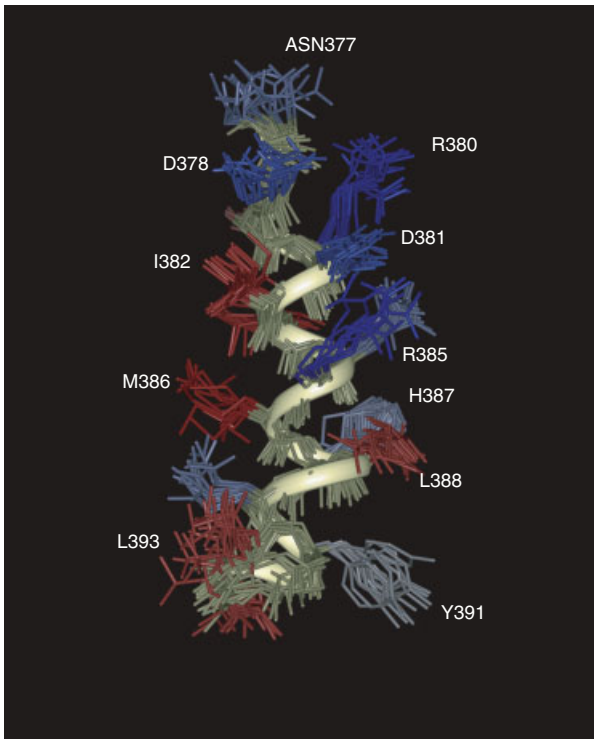

Plate 2 Backbone superposition of residues Asn^{377}-Leu^{394} of Gα_s(374–394)C^{379}A structures collected every 5 ps during the last 50 ps of a molecular dynamics simulation. Amino acid side chains are coloured according to their hydrophobic character. High, medium and low hydrophobic residues are coloured in red, grey/light-blue and blue respectively.

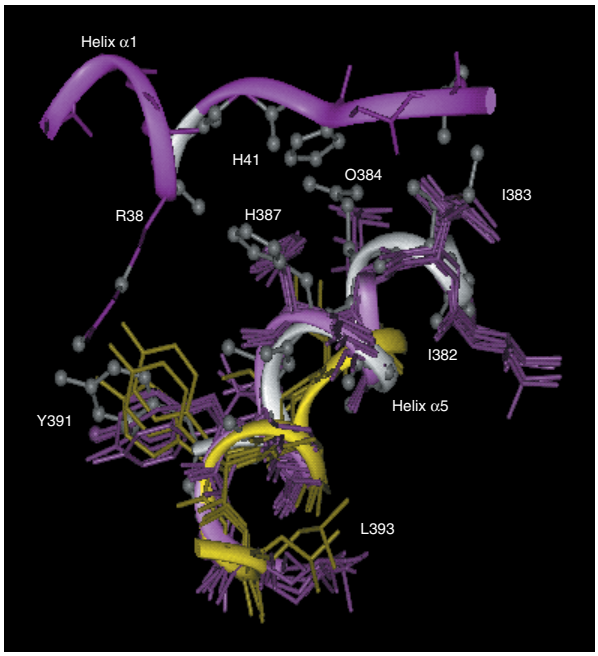

Plate 3 Backbone conformations of Gα_s(380–394) (yellow) and Gα_s(374–394)C^{379}A (purple) superimposed on the crystallographic structure of the same fragment in the Gα_s protein (grey ribbon) [26] named helix α5 in the 1AZT PDB file. A ribbon representation of the helix α1 of the protein is also displayed (1AZT PDB file). The atoms of the crystal model included in a range of 5 Å from helix α5 are coloured grey and represented with stick and ball render.

up of five *C*-terminal residues in the 11-mer peptide and 11 *C*-terminal residues in the 21-mer peptide. Our previous results suggest a dependence of the biological activity on the size of the peptides and on their content of ordered secondary structure [21, 29]. Nevertheless, the non linearity of biological data suggests that the backbone secondary structure is not the only factor ruling the effectiveness of the biological activity.

On the basis of these data and to better understand the mechanistic principles connecting biological activity and structural properties, we have extended our NMR studies of the $G\alpha_s$ *C*-terminal peptides to the15-residue $G\alpha_s$(380–394).

CD and NMR data of $G\alpha_s$(380–394) were collected in water, water/methanol and water/HFA mixtures. Due to the prevalence of water in the majority of biological compartments, water seems to be the most biocompatible medium in which to perform solution conformational studies. Unfortunately, under these conditions it is very difficult to build a 3D-model of linear peptides of small dimension due to the flexibility that hinders the collection of an adequate number of NOE effects to be used as distance restraints for the structural calculations. This problem can be overcome using solvent mixtures with a viscosity higher than that of pure water, able to favour ordered, more compact conformers over extended and/or disordered ones. Alcohols, either neat or mixed with water, are the most popular media used to induce 'environmental constraints' in peptides [46]. Since their physicochemical properties are for some aspects comparable to those of biological fluids, they can be considered as biomimetic environments and, in many cases, they have been shown not to interfere with the normal biological activity [47,48]. In addition to common alcohols, mixtures of water with fluorinated solvents are used [49,50]. The TFE/water mixture is the most widely known helix-inducing medium, but recently an HFA/water mixture has been shown to be endowed of a much higher helix-inducing propensity [40,41]. Such a propensity, however, does not override the intrinsic tendency dictated by the sequence of specific residues, as shown by the structure of β-endorphin in which a long helical segment coexists with a random coil stretch [51].

The CD spectra of $G\alpha_s$(380–394) in water are consistent with a completely unordered structure. The data collected in water/methanol, although showing several interesting NOEs, do not define a complete pattern suitable as a starting point for the calculation of a 3D model. Indeed we limited the quantitative NMR study of $G\alpha_s$(380–394) to the HFA/water solution. NMR spectra of $G\alpha_s$(380–394) (Figure 4), recorded in such a mixture, defined a NOE pattern that corresponded to an α-helix structure extending from $G\alpha_s$ Ile^{382} to Leu^{393} with a decrease of regularity at residue Leu^{388} (Plates 1a and 2). The extension of the *C*-terminal helix of the 15-mer confirms that, despite a non-linear dependence of the biological activity on the size of the peptides, a proportionality exists between the content of ordered secondary structure and the size of the peptides. This is clearly evident in Plate 1b where the overlapping of the NMR structures of the 15-mer and the 21-mer as well as the good agreement between the NMR and the crystal structures are observable.

The role played by the side-chain orientation in generating contacts critical for receptor G protein interactions has been evidenced by a wealth of experimental data [3, 6, 8, 10, 12] as well as by theoretical models based on the analysis of the primary structure of both the G protein α subunit and G protein coupled receptor [21]. Recently, a low resolution model of receptor/G protein coupling has been elaborated by Oliveira *et al.* on the basis of possible interactions occurring between highly conserved residues of both G protein and receptors [21].

According to this model, a dipolar interaction between two Asp residues in helix α5 of the Gα subunit and the Arg residue in the DRY motif (conserved in 99% of receptors) of the transmembrane domain III of a receptor could represent a key event driving all coupling processes.

To investigate the role of the side-chain arrangement in affecting the functionality of the *C*-terminal peptides, we explored their conformational space by molecular dynamics calculations. The final derived structures are characterized by side chains with well-defined orientations (Plate 2). An analysis of the side chains according to their hydrophobic character suggests that a polar surface can be identified due to the presence of charged residues Asp^{378}, Asp^{381}, and Arg^{380}, Arg^{385}. On the other hand, two hydrophobic surfaces are defined by residues exhibiting less polar side chains (His^{387}, Tyr^{391}) and apolar side chains (Ile^{382}, Ile^{383}, Met^{386}, Leu^{393}).

The conformations of some highly conserved residues of $G\alpha_s$ *C*-terminal peptides (Val^{375}, Phe^{376}, Asp^{378}, Asp^{381}, Ile^{383}, Leu^{388} and Leu^{393}) were analysed according to the previously mentioned model of Oliveira *et al.* [21]. Concerning Asp^{378} and Asp^{381}, it is interesting to note that they are both included

in the sequence of the 21-mer $G\alpha_s(374–394)C^{379}A$ peptide, where they appear structurally defined and correctly exposed to undertake contacts with a positive charged residue on the receptor. By contrast, $G\alpha_s(380–394)$ lacks Asp^{378} in its sequence and contains Asp^{381} in a position located on the border of its coil *N*-terminal portion. This finding implies that the crucial interactions involving the two Asp residues could not take place in the case of the 15-mer peptide $G\alpha_s(380–394)$. These data emphasize the important role of the side chains in determining the biological profile of the different fragments considered in the present study [20]. This is a particularly relevant observation in the context of the G protein/receptor system, where the factors determining the selectivity or the promiscuity of the coupling are still under investigation.

In their model Oliveira *et al.* [21] have also proposed that the formation of a multi-helix interaction between the *C*- and *N*-terminal helices (helix $\alpha1$ and helix $\alpha5$) of the $G\alpha$ subunits and the *C*-terminal helix of the receptor is important to maintain correct communication between receptors and G proteins. Accordingly, it is interesting to compare our models with the crystal structure of $G\alpha_s$ protein (ref. code 1AZT) [26]. In Plate 3 the models of the 15-mer and 21-mer $G\alpha_s$ peptides are overlapped to the corresponding region of the $G\alpha_s$ crystal structure (helix $\alpha5$). The interaction between helix $\alpha5$ and helix $\alpha1$ of the crystal model is also shown [26]. The side chains responsible for the interaction between the two helices in the crystal fit well with those lining one of the two hydrophobic surfaces found in the NMR structures. Accordingly, His^{387} and Tyr^{391} of the $G\alpha_s$ *C*-terminus calculated models are correctly oriented to interact with helix $\alpha1$ through an intramolecular interaction (Plate 3) as observed in the crystal structure of the $G\alpha_s$ protein. In addition, the second hydrophobic surface defined by the side chains of Leu^{393}, Met^{386} and Ile^{382} seems to have an orientation suitable for contacts with the *C*-terminal helix of the cognate receptor (Plate 3).

Another important issue to be analysed is the subtype specificity of the G protein/receptor interaction. An alignment of the sequences of the *C*-terminal regions of $G\alpha_s$ proteins (Figure 5) indicates typical residues such as Asn^{377}, Asp^{378}, Cys^{379}, Gln^{384}, Met^{386}, His^{387} and Glu^{392}. Many of these residues are charged, at variance with the corresponding residues of other $G\alpha$ subunits (Figure 5). From a structural point of view it is also interesting that these polar/charged residues, that usually favour solvating interactions and destabilize ordered secondary structures, have defined orientations that contribute to the stability of the secondary structure and produce the correct orientation for specific interactions with the receptor. The role of these peculiar residues is now under investigation in an attempt to clarify the specificity of the interaction that many lines of experimental evidence suggest.

Protein	n	ID	aa	aa Sequence										
Gt	b	P04695	330-350	F	VF	DAVT	D	I	I	IKEN	L	KDCGL	L	F
Gs	b	RGBOGA	374-394	R	VF	NDCR	D	I	I	QRMH	L	RQYEL	L	L
Gi1	b	RGBOI1	334-354	F	VF	DAVT	D	I	I	IKNN	L	KDCGL	L	F
Go	b	P08239	334-354	V	VF	DAVT	D	I	I	IANN	L	RGCGL	L	Y
Gq	h	2204262A	339-359	F	VF	AAVK	D	I	I	LQLN	L	KEYNL	L	V
Gz	h	P19086	335-355	F	VF	DAVT	D	I	I	IQNN	L	KYIGL	L	C
Gi3	h	M20597	334-354	F	VF	DAVT	D	I	I	IKNN	L	KECGL	L	Y
Golf	r	P38406	361-381	R	VF	NDCR	D	I	I	QRMH	L	KQYEL	L	L
G12	m	P27600	359-379	F	VF	HAVK	D	I	I	LQEN	L	KDIML	L	Q
G15	m	P30678	354-374	S	VF	KDVR	D	S	V	LARY	L	DEINL	L	L
G13	m	B41095	357-377	F	VF	RDVK	D	T	I	LHDN	L	KQLML	L	Q
G14	m	A41534	335-355	F	VF	AAVK	D	T	I	LQLN	L	REFNL	L	V

Figure 5 Amino acid sequence comparison of the last 21 *C*-terminal residues of G protein α subunits. Conserved Val^{375}, Phe^{376}, Asp^{381}, Ile^{383}, Leu^{388} and Leu^{393} are shaded and outlined. Protein sources: b, bovine; h, human; m, mouse; r, rat. Full protein sequences are available from the National Center for Biotechnology Information at http://www.ncbi.nlm.nih.gov/Entrez/protein.html.

CONCLUSIONS

The main goal of our conformational study of *C*-terminal peptides was an investigation of the structural factors affecting the strength of the interaction of the $G\alpha_s$ subunit with the receptor, in particular the stability of the helical stretch, its length and the specific arrangement of side chains. The prevailing conformation of $G\alpha_s(380–394)$, examined by NMR spectroscopy in a mixture of HFA/water, exhibits a significantly long helical stretch. If the biological activity of the peptide is not proportional to the content of the helical structure, the low ordered conformation of the side chains considered essential for G protein/receptor coupling could account for the weak activity of this peptide. Consistently, the significant activity of $G\alpha_s(374–394)C^{379}A$ is in line with the observation that this peptide maintains all the key contacts postulated in the G protein/receptor interaction. In particular, characteristic charged residues are correctly exposed to interact specifically with the receptor.

Acknowledgements

This work was supported by a Human Capital and Mobility grant (CHRX-CT94-0689) from the European Community, Regione Campania (POP 1996–2000) and Ministero Università Ricerca Scientifica e Tecnologica (PRIN 2000).

REFERENCES

1. Hamm HE. The many faces of G protein signal. *J. Biol. Chem.* 1998; **273**: 669–672.
2. Freissmuth M, Waldhoer M, Bofill-Cardona E, Nanoff C. G protein antagonists. *Trends Pharmacol. Sci.* 1999; **20**: 237–245.
3. Conklin BR, Farfel Z, Lustig KD, Julius D, Bourne HR. Substitution of three amino acids switches receptor specificity of $G_q\alpha$ to that of $G_i\alpha$. *Nature* 1993; **363**: 274–276.
4. Conklin BR, Herzmark P, Ishida S, Voyno-Yasenetskaya TA, Sun Y, Farfel Z, Bourne HR. Carboxyl-terminal mutations of Gq_α and Gs_α that alter the fidelity of receptor activation. *Mol. Pharmacol.* 1996; **50**: 885–890.
5. Onrust R, Herzmark P, Chi P, Garcia PD, Lichtarge O, Kingsley C, Bourne HR. Receptor and β,γ-binding sites in the α-subunit of the retinal G protein transducin. *Science* 1997; **275**: 381–384.
6. Kostenis E, Conklin BR, Wess J. Molecular basis of receptor/G protein coupling selectivity studied by coexpression of wild type and mutant m2 muscarinic receptors with mutant $G\alpha_q$ subunits. *Biochemistry* 1997; **36**: 1487–1495.
7. Kostenis E, Gomeza J, Lerche C, Wess J. Genetic analysis of receptor-$G\alpha_q$ coupling selectivity. *J. Biol. Chem.* 1997; **272**: 23 675–23 681.
8. Kostenis E, Zeng F, Wess J. Functional characterization of a series of mutant G protein α_q subunits displaying promiscuous receptor coupling properties. *J. Biol. Chem.* 1998; **273**: 17 886–17 892.
9. Marsh SR, Grishina G, Wilson PT, Berlot CH. Receptor-mediated activation of $G_{s\alpha}$: evidence for intramolecular signal transduction. *Mol. Pharmacol.* 1998; **53**: 981–990.
10. Grishina G, Berlot CH. A surface-exposed region of $G_{s\alpha}$ in which substitutions decrease receptor-mediated activation and increase receptor affinity. *Mol. Pharmacol.* 2000; **57**: 1081–1092.
11. Bae H, Anderson K, Food LA, Skiba NP, Hamm HE, Graber SG. Molecular determinants of selectivity in 5-hydroxytryptamine$_{1B}$ receptor-G protein interactions. *J. Biol. Chem.* 1997; **272**: 32 071–32 077.
12. Bae H, Cabrera-Vera TM, Depree KM, Graber SG, Hamm HE. Two amino acids within the α4 helix of $G\alpha_{i1}$ mediate coupling with 5-hydroxytryptamine$_{1B}$ receptors. *J. Biol. Chem.* 1999; **274**: 14 963–14 971.
13. Hamm HE, Deretic D, Arendt A, Hargrave PA, Konig B, Hofmann KP. Site of G protein binding to rhodopsin mapped with synthetic peptides from the α subunit. *Science* 1988; **241**: 832–835.
14. Kisselev OG, Ermolaeva MV, Gautam N. A farnesylated domain in the G protein γ-subunit is a specific determinant of receptor coupling. *J. Biol. Chem.* 1994; **2692**: 21 399–21 402.
15. Rasenick MM, Watanabe M, Lazarevic MB, Hatta S, Hamm HE. Synthetic peptides as probes for G protein function: carboxyl-terminal $G\alpha_s$ peptides mimic G_s and evoke high affinity agonist binding to β-adrenergic receptors. *J. Biol. Chem.* 1994; **269**: 21 519–21 525.
16. Kisselev O, Pronin A, Ermolaeva M, Gautam N. Receptor-G protein coupling is established by a potential conformational switch in the $\beta\gamma$ complex. *Proc. Natl Acad. Sci. USA* 1995; **92**: 9102–9106.
17. Kisselev O, Ermolaeva M, Gautam N. Efficient interaction with a receptor requires a specific type of prenyl group on the G protein γ-subunit. *J. Biol. Chem.* 1995; **270**: 25 356–25 358.
18. Gilchrist A, Mazzoni MR, Dineen B, Dice A, Linden J, Proctor WR, Lupica CR, Dunwiddie TV, Hamm HE. Antagonists of the receptor-G protein interface block G_i-coupled signal transduction. *J. Biol. Chem.* 1998; **273**: 14 912–14 919.
19. Kisselev OG, Meyer CK, Heck M, Ernst OP, Hofmann KP. Signal transfer from rhodo n to the G-protein: evidence for a two-site sequential fit mechanism. *Proc. Natl Acad. Sci. USA* 1999; **96**: 4898–4903.
20. Mazzoni MR, Taddei S, Giusti L, Rovero P, Galoppini C, D'Ursi AM, Albrizio S, Triolo A, Novellino E,

Greco G, Lucacchini A, Hamm HE. A Ga_s carboxyl-terminal peptide prevents G_s activation by the A_{2A} adenosine receptor. *Mol. Pharmacol.* 2000; **58**: 226–236.
21. Oliveira L, Paiva ACM, Vriend G. A low resolution model for the interaction of G proteins with G protein-coupled receptors. *Protein Eng.* 1999; **12**: 1087–1095.
22. Noel J, Hamm HE, Sigler PB. The 2.2 Å crystal structure of transducin-α complexed with GTPγs. *Nature* 1993; **366**: 654–663.
23. Lambright DG, Noel JP, Hamm HE. Structural determinants for the activation of the α-subunit of a heterotrimeric G protein. *Nature* 1994; **369**: 621–628.
24. Coleman DE, Berghuis AM, Lee E, Linder ME, Gilman GA, Sprang SR. Structure of active conformations of $G_{i\alpha 1}$ and the mechanism of GTP hydrolysis. *Science* 1994; **265**: 1405–1412.
25. Mixon MB, Lee E, Coleman DE, Berghuis AM, Gilman AG, Sprang SR. Tertiary and quaternary structural changes in $G_{i\alpha 1}$ induced by GTP hydrolysis. *Science* 1995; **270**: 954–960.
26. Sunahara RK, Tesmer JJG, Gilman AG, Sprang SR. Crystal structure of the adenylyl cyclase activator $G_{s\alpha}$. *Science* 1997; **278**: 1943–1947.
27. Dratz EA, Gisachew Busse SC, Rens-Domiano S, Hamm HE. NMR structure of a receptor bound G-protein peptide: structure refinement and update. *Biophys. J.* 1996; **70**: A16.
28. Kisselev OG, Kao J, Ponder JW, Fann YC, Gautam N, Marshall GR. Light-activated rhodopsin induces structural binding motif in G protein α-subunit. *Proc. Natl Acad. Sci. USA* 1998; **95**: 4270–4275.
29. Albrizio S, D'Ursi AM, Fattorusso C, Galoppini C, Greco G, Mazzoni MR, Novellino E, Rovero P. Conformational studies on a synthetic *C*-terminal fragment of the α-subunit of G_s proteins. *Biopolymers* 2000; **54**: 186–194.
30. Piantini U, Sorensen OW, Ernst RR. Multiple quantum filters for elucidating NMR coupling network. *J. Am. Chem. Soc.* 1982; **104**: 6800–6801.
31. Bax A, Davis DG. Practical aspect of two-dimensional transverse NOE spectroscopy. *J. Magn. Reson.* 1985; **63**: 207–213.
32. Jeener J, Meyer BH, Bachman P, Ernst RR. Investigation of exchange processes by two-dimensional NMR spectroscopy. *J. Chem. Phys.* 1979; **71**: 4546–4553.
33. Marion D, Wühtrich K. Application of phase sensitive two-dimensional correlated spectroscopy (COSY) for measurements of ^{1}H-^{1}H spin-spin coupling constants in proteins. *Biochem. Biophys. Res. Commun.* 1983; **113**: 967–974.
34. Bartels C, Xia T, Billeter M, Guentert P, Wüthrich K. The program XEASY for computer-supported NMR spectral analysis of biological macromolecules. *J. Biomol. NMR* 1995; **6**: 1–10.
35. Guntert P, Mumenthaler C, Wüthrich K. Torsion angle dynamics for NMR structure calculation with the new program DYANA. *J. Mol. Biol.* 1997; **273**: 283–298.
36. Case DA, Pearlman DA, Caldwell JW, Cheatham IIITE, Ross WS, Simmerling CL, Darden TA, Merz KM, Stanton RV, Cheng AL, Vincent JJ, Crowley M, Ferguson DM, Radmer RJ, Seibel GL, Singh UC, Weiner PK, Kollman PA. *AMBER 5*, 1997; University of California, San Francisco.
37. Pearlman DA, Case DA, Caldwell JW, Ross WS, Cheatham IIITE, DeBolt S, Ferguson D, Seibel G, Kollman PA. AMBER, a package of computer programs for applying molecular mechanics, normal mode analysis, molecular dynamics and free energy calculations to simulate the structural and energetic properties of molecules. *Comput. Phys. Commun.* 1995; **91**: 1–41.
38. Laskowski RA, Rullmann JA, MacArthur MW, Kaptein R, Thornton JM. AQUA and PROCHECK-NMR: programs for checking the quality of protein structures solved by NMR. *J. Biomol. NMR* 1996; **8**: 477–486.
39. MSI Molecular Symulations, 9685 Scranton Road, San Diego, CA 92121-3752, USA.
40. Rajan R, Awasthi SK, Bhattacharjya S, Balaram P. 'Teflon-coated peptides': hexafluoroacetone trihydrate as a structure stabilizer for peptides. *Biopolymers* 1997; **42**: 125–128.
41. Rajan R, Balaram P. A model for the interaction of trifluoroethanol with peptides and proteins. *Int. J. Pept. Protein Res.* 1996; **48**: 328–336.
42. Johnson WC, Jr. Protein secondary structure and circular dichroism: a practical guide. *Proteins: Structure Function Gen.* 1990; **7**: 205–214.
43. Wüthrich K. *NMR of Proteins and Nucleic Acids*. Wiley: New York, 1986.
44. Wishart DS, Sykes BD, Richards FM. Relationship between nuclear magnetic resonance chemical shift and protein secondary structure. *J. Mol. Biol.* 1991; **222**: 311–333.
45. Wishart DS, Sykes BD, Richards FM. The chemical shift index: a fast and simple method for the assignment of protein secondary structure through NMR spectroscopy. *Biochemistry* 1992; **31**: 1647–1651.
46. Picone D, D'Ursi A, Motta A, Tancredi T, Temussi PA. Conformational preferences of [Leu5]enkephalin in biomimetic media. Investigation by ^{1}H NMR. *Eur. J. Biochem.* 1990; **192**: 433–439.
47. Douzou P, Petsko GA. Proteins at work: 'stop-action' pictures at subzero temperatures. *Adv. Protein Chem.* 1984; **36**: 245–361.
48. Fink AL. Protein folding in cryosolvents at subzero temperatures. *Methods Enzymol.* 1986; **131**: 173–187.
49. Shiraki K, Nishikawa K, Goto Y. Trifluoroethanol-induced stabilization of the α-helical structure of β-lactoglobulin: implication for non-hierarchical protein folding. *J. Mol. Biol.* 1995; **254**: 180–194.

50. Sonnichsen FD, Van Eyk JE, Hodges RS, Sykes BD. Effect of trifluoroethanol on protein secondary structure: an NMR and CD study using a synthetic actin peptide. *Biochemistry* 1992; **31**: 8790–8798.

51. Saviano G, Crescenzi O, Picone D, Temussi PA, Tancredi T. Solution structure of human β-endorphin in helicogenic solvents: A NMR study. *J. Pept. Sci.* 1999; **5**: 410–422.

